The Impact of Satellite Winds on Experimental GFDL Hurricane Model Forecasts

BRIAN J. SODEN

Geophysical Fluid Dynamics Laboratory, National Oceanic and Atmospheric Administration, Princeton, New Jersey

CHRISTOPHER S. VELDEN

Cooperative Institute for Meteorological Satellite Studies, University of Wisconsin—Madison, Madison, Wisconsin

ROBERT E. TULEYA

Geophysical Fluid Dynamics Laboratory, National Oceanic and Atmospheric Administration, Princeton, New Jersey

(Manuscript received 12 April 2000, in final form 22 August 2000)

ABSTRACT

A series of experimental forecasts are performed to evaluate the impact of enhanced satellite-derived winds on numerical hurricane track predictions. The winds are derived from *Geostationary Operational Environmental Satellite-8* (*GOES-8*) multispectral radiance observations by tracking cloud and water vapor patterns from successive satellite images. A three-dimensional optimum interpolation method is developed to assimilate the satellite winds directly into the Geophysical Fluid Dynamics Laboratory (GFDL) hurricane prediction system. A series of parallel forecasts are then performed, both with and without the assimilation of GOES winds. Except for the assimilation of the satellite winds, the model integrations are identical in all other respects. A strength of this study is the large number of experiments performed. Over 100 cases are examined from 11 different storms covering three seasons (1996–98), enabling the authors to account for and examine the case-to-case variability in the forecast results when performing the assessment. On average, assimilation of the GOES winds leads to statistically significant improvements for all forecast periods, with the relative reductions in track error ranging from ~5% at 12 h to ~12% at 36 h. The percentage of improved forecasts increases following the assimilation of the satellite winds, with roughly three improved forecasts for every two degraded ones. Inclusion of the satellite winds also dramatically reduces the westward bias that has been a persistent feature of the GFDL model forecasts, implying that much of this bias may be related to errors in the initial conditions rather than a deficiency in the model itself. Finally, a composite analysis of the deep-layer flow fields suggests that the reduction in track error may be associated with the ability of the GOES winds to more accurately depict the strength of vorticity gyres in the environmental flow. These results offer compelling evidence that the assimilation of satellite winds can significantly improve the accuracy of hurricane track forecasts.

1. Introduction

Numerical prediction of hurricane forecasts requires accurate representation of the current meteorological conditions. Unfortunately, conventional measurements used to initialize forecast models are unavailable for vast areas of the tropical oceans. The sparsity of observations, both near the storm center and in the surrounding environment, is a key factor in limiting the accuracy of hurricane forecasts (Burpee et al. 1984, 1996; Aberson and Franklin 1999). Several studies have demonstrated that the inclusion of near-storm observations can substantially improve hurricane forecasts. For example, Franklin and DeMaria (1992) found statistically significant improvements in the predicted storm tracks when dropwindsonde observations were included in a barotropic model. Likewise, in a study using the National Centers for Environmental Prediction (NCEP) global forecast model, Lord (1993) demonstrated a reduction in track error of ~25% due to the inclusion of dropwindsonde measurements. Using the Geophysical Fluid Dynamics Laboratory (GFDL) hurricane model, Tuleya and Lord (1997) reduced forecast track errors by up to 30% when dropwindsonde data were assimilated into the model. More recently, Aberson and Franklin (1999) also found improvements in the GFDL model track forecasts after including dropwindsonde data. Burpee et al. (1996) provide a summary of recent improvements in hurricane track forecasts due to the assimilation of dropwindsonde data.

Corresponding author address: Dr. Brian J. Soden, Geophysical Fluid Dynamics Laboratory, National Oceanic and Atmospheric Administration, P.O. Box 308, Princeton, NJ 08542.
E-mail: bjs@gfdl.gov

In addition to dropwindsonde measurements, atmospheric winds over data-void regions of the oceans can also be derived by tracking cloud and water vapor features in geostationary satellite imagery. The ability to provide high-density wind coverage over large regions of the Tropics makes satellite winds particularly useful for studying tropical cyclones (Velden et al. 1998; LeMarshall 1998). Although satellite-derived winds have been produced operationally for more than a decade, recent enhancements in spatial resolution and radiometric sensitivity from the new generation of Geostationary Operational Environmental Satellites (GOES) have significantly improved both the accuracy and density of the wind products (Velden et al. 1997). Yet despite their obvious utility for measuring tropical winds, there have been relatively few attempts to determine the impact of GOES winds on numerical hurricane track forecasts, particularly for the Atlantic. Velden et al. (1992) demonstrated that the assimilation of satellite winds into the VICBAR model resulted in modest (2%–6%) reductions in the mean track error, although none of the improvements were considered to be statistically significant. Leslie et al. (1998) demonstrated that the assimilation of high-density satellite winds can greatly improve track forecasts in a high-resolution model, although their study was limited to only two cases. Recently, Goerss et al. (1998) examined the impact of an experimental high-density GOES wind product on hurricane track predictions from the Navy Oceanographic Global Atmospheric Prediction System (NOGAPS) forecast model. Based upon results from four tropical Atlantic storms from the 1995 season, this study found that assimilation of the experimentally derived GOES winds reduced the track errors in the NOGAPS model by 12%–14%. Consequently, operational assimilation of these winds into the NOGAPS model was initiated in 1996 and has continued since.

In recent years one of the most accurate models for predicting hurricane tracks has been the GFDL Hurricane Prediction System (Kurihara et al. 1998). In contrast to the NOGAPS model, the GFDL Hurricane Prediction System uses a limited-area, multiply nested model designed specifically for tropical cyclone prediction. Given these distinctions, and in light of its demonstrated skill in track prediction, this study seeks to determine the extent to which GFDL model forecasts can benefit from the direct assimilation of GOES winds. Toward this end, a series of over 100 parallel forecasts (with and without GOES winds) were performed spanning 11 storms and three Atlantic hurricane seasons (1996–98). Section 2 provides brief descriptions of the GFDL hurricane prediction system, the GOES wind dataset, and the analysis method used to assimilate the GOES winds into the GFDL model. Section 3 presents the results of selected individual cases, as well as statistical summaries of forecast improvements. A discussion of the implications of these results and objectives for future research is provided in section 4.

2. Description of the forecast model, observational data, and assimilation method

a. Forecast model: The GFDL Hurricane Prediction System

The dynamical model used in the hurricane prediction system is an outgrowth of a research model developed at GFDL and adopted by the National Weather Service as an operational hurricane forecast model in 1995. A brief summary of its distinctive features is provided here; a more complete description can be found in Kurihara et al. (1998) and references therein. The prediction system uses a limited area, three-dimensional model that solves the primitive equations using a finite-difference method in spherical coordinates with 18 vertical levels in sigma coordinates. To resolve the interior structure of a hurricane, a multiply nested grid system is used consisting of two inner movable meshes ($\frac{1}{6}°$ and $\frac{1}{3}°$ resolution) nested within a coarser $75° \times 75°$ outer mesh (1° resolution). The outer nest remains geographically fixed during a forecast, while the inner two nests remain centered on the storm. Further details on the nested grid system are provided in Kurihara et al. (1998).

The initial and lateral boundary conditions are defined by the NCEP global analysis and prediction model. Tropical cyclone structure information is determined from the National Hurricane Center (NHC) storm message. The global NCEP analyses (1° resolution) are spatially interpolated onto the two inner nested regional domains of the model. To produce realistic storm-scale circulations near the center of the hurricane, a synthetic vortex specification procedure is used that is compatible with the nested mesh model (Kurihara et al. 1993). After insertion of the idealized vortex, small adjustments are made to the surface pressure and temperature fields to minimize imbalances with the existing wind field by solving the reverse balance equation (Kurihara et al. 1995). The resulting wind, mass, and thermodynamic fields provide the initial conditions for the nested model forecast. The model is then integrated for 72 h yielding both track and intensity forecasts. These steps are summarized in Fig. 1. It is important to note that since 1996 NCEP has routinely included any available dropwindsonde data from aircraft flights into the global analysis. Hence, the background field used for both the control and satellite-wind experiments already contains the improvements resulting from these additional observations for cases in which they were available. The high-density GOES winds, however, were not included until 1998 (see section 3.4). For the satellite-wind experiments, a three-dimensional optimum interpolation (3DOI) scheme (described below) is used to assimilate the GOES winds into the outermost (1°) grid using the NCEP analyses as the first-guess field. Once the GOES winds have been assimilated, the model initialization procedure is identical to that described above. Namely, the assimilated wind fields are interpolated from the

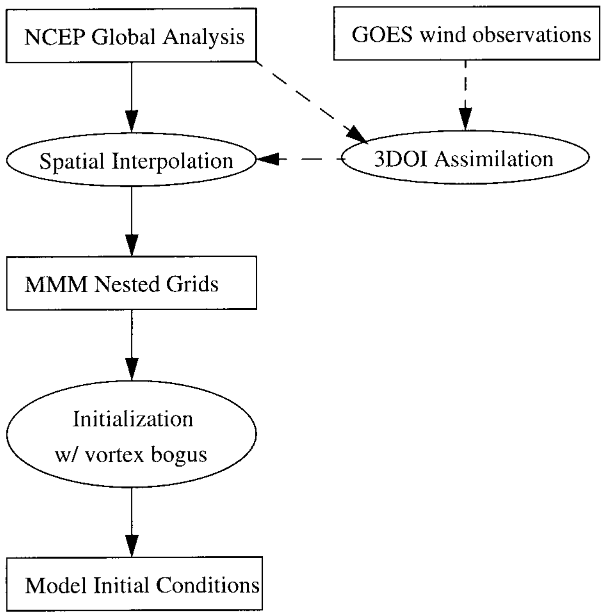

FIG. 1. An outline of the steps for determining the initial conditions in the GFDL Hurricane Prediction System after Kurihara et al. (1998). Dashed arrows indicate the additional steps performed for the WIND experiments.

outer grid onto the two inner nested grids, the synthetic vortex is added, and the mass and winds fields are rebalanced following Kurihara et al. (1995).

b. Observational dataset: GOES high-density multispectral winds

This section provides a brief overview of the GOES processing algorithm used to derive the satellite winds used in this study. Starting in 1996, experimental wind datasets derived from GOES observations have been produced at the Cooperative Institute for Meteorological Satellite Studies (CIMSS) at the University of Wisconsin—Madison. An automated procedure uses cross-correlation techniques to track cloud and water vapor structures from sequential satellite imagery. Tropospheric motions inferred from successive satellite images (15–30-min intervals) are used to estimate winds at multiple levels using multispectral imagery. Successfully tracked vectors are assigned heights based upon an optimal match between the observed radiance and a corresponding temperature profile. The content of the satellite-derived winds are optimized using an objective quality control and automated processing system described by Velden et al. (1998). High-resolution visible (0.6 μm) imagery is used to track shallow cumulus clouds in the lower troposphere (600–900 hPa). These low-level winds are complemented by vectors produced from infrared (11 μm) window imagery, particularly in the cirrus-laden outflow regions of the upper troposphere. In clear regions tropospheric motions are derived by tracking water vapor structures observed in GOES water vapor channels. These channels, located at 6.7, 7.0, and 7.3 μm, sense different portions of the water vapor absorption band and are used to track thin layers of moisture in the upper (e.g., 150–350 hPa) and middle troposphere (e.g., 350–550 hPa).

Illustrations of the typical horizontal and vertical coverage obtained by the advanced GOES winds and further details regarding their derivation are provided by Velden et al. (1998) and references therein.

c. Data assimilation: Three-dimensional optimum interpolation

As noted in the introduction, the majority of hurricane impact studies have focused on the assimilation of conventional data, such as dropwindsondes, which provide a relatively complete vertical profile of the wind field. The GOES winds, on the other hand, are distinguished by their broad spatial coverage but traditionally have offered relatively poor vertical resolution and vertical sampling. While the limited vertical sampling has been partially mitigated by the inclusion of water vapor winds, these winds still present some unique challenges for effectively incorporating them into a forecast model. These challenges have likely contributed to the relative lack of attention such data have received. For the present study, a 3DOI scheme was developed to assimilate the satellite winds directly into the GFDL model. Previous studies (Goerss et al. 1998) have shown that 3DOI methods can be used to effectively assimilate GOES winds into numerical models. While there are more sophisticated tools for data assimilation, such as four-dimensional variational analysis (4DVAR), the primary focus of this study is to evaluate the impact of the GOES winds on the GFDL model forecasts, not to develop the optimal strategy for assimilating the data. This analysis scheme is not intended to be implemented operationally, but rather to provide a simple means for directly evaluating the sensitivity of hurricane forecasts to additional satellite data. However, we recognize that the impact of the data will depend to some degree upon the assimilation strategy employed. Indeed, it is reasonable to assume that a more sophisticated assimilation method, such as one that could include the high time and space resolution of the satellite data and account for time variations of the error field (i.e., 4DVAR), would likely yield better results (e.g., Leslie et al. 1998). Therefore the positive impacts demonstrated here may be considered to represent a *lower bound* on the potential of GOES winds to improve track forecasts.

The 3DOI scheme developed for this study is similar to that described by Goerss and Phoebus (1992). Since the concept of optimum interpolation dates back to Gandin (1963), only a brief discussion of the method is provided here. Further details can be found in Theibaux and Pedder (1987), Daley (1991), and others. The first step in the assimilation procedure is to determine the increment field, defined as the difference between the observed (GOES) and first-guess (NCEP global analysis) winds for each observation. GOES observations, valid at the same synoptic time as the first-guess (0000 and 1200 GMT), are subtracted from the first-guess field by spatially interpolating the first-guess field (bilinearly in the horizontal and linear in log pressure in the vertical) to the location of the GOES observations. Since there are typically several thousand observations at any given time, it is necessary to reduce the observational data volume to yield a computationally efficient analysis. For this purpose, ''superobservations'' are created by linearly averaging the wind increments within each grid volume (i.e., each $1° \times 1°$ horizontal square and each layer) of the first-guess field to create a single superobservation increment. This procedure typically reduces the number of observations to be assimilated by roughly a factor of 4. The analyzed field is then computed by adding a finite number, N, of optimally weighted increments to the first-guess field,

$$F_k^a = F_k^g + \sum_{i=1}^{N} w_{ik} f_i^o, \quad (1)$$

where F represents a total-field wind component and f represents an incremental wind component. The superscripts a, g, and o denote the analyzed, first-guess, and observed values, respectively. The subscript k denotes the location of the analyzed (and first guess) field, while the subscript i denotes an observation location. To yield a computationally efficient analysis, the maximum number of observations (N) used in the analysis for each grid point k is 30. They are determined by selecting the 30 observation locations for which the first-guess error is most strongly correlated with the grid point being analyzed, based upon an assumed error covariance model (see below). The error in the analyzed field, ε, is then determined as a weighted combination of errors in the first-guess field, δF_k^g, and increment field, δf_i^o,

$$\varepsilon_k = \delta F_k^g + \sum_{i=1}^{N} w_{ik} \delta f_i^o. \quad (2)$$

Provided that the statistics of the first-guess and observational error are known, the 3DOI method yields the optimal set of weights, w_{ik}, for each superobservation and analysis grid. The weights are optimal in the sense that they minimize the mean square error of the analysis,

$$\frac{\partial}{\partial w_{ik}} \varepsilon_k^2 = 0 \qquad i = 1, N. \quad (3)$$

The above requirement yields a set of N linear equations,

$$\mathbf{w}_k = \mathsf{M}^{-1}\mathbf{h}_k, \quad (4)$$

where $\mathbf{w}_k$ is an N-dimensional vector of weights and $\mathbf{h}_k$ is an N-dimensional row vector of the first-guess error covariance between the N observation locations i and the analysis grid point location k. The square ($N \times N$) matrix, M, contains the covariance of the first-guess error between each location i and the other $N - 1$ locations. To account for errors in the observations, a factor $1/\gamma$ is added to the diagonal terms of M, where γ is the ratio of the signal variance to noise variance of the observations (Theibaux and Pedder 1987). For the GOES winds, a signal-to-noise ratio of 8:1 is assumed here based on the error characteristics of the GOES winds (Velden et al. 1998). Following convention, this formulation also assumes that the error associated with each individual observation is uncorrelated with the first-guess errors and with all other observations. The only quality control that is performed during the assimilation is to reject water vapor winds located below 300 hPa. This is done due to the uncertainty in determining the thickness of the moisture layer corresponding to the pure water vapor wind vectors.

A key aspect of any statistical analysis is providing an accurate description of the error covariance in the first-guess field. For the purposes of this study, a simple analytical covariance model is used in which the error variance for both the first-guess and observed fields is assumed to be constant at all locations and their space lag covariances are horizontally isotropic. This permits M and $\mathbf{h}_k$ to be expressed in terms of idealized correlation functions. Accordingly, the three-dimensional error correlation in the first-guess field is expressed as the product of the horizontal (ρ^{xy}) and vertical (ρ^z) error correlations, $\rho = \rho^{xy}\rho^z$. Both correlation functions are assumed to be invariant in space and time and are expressed in terms of the horizontal (Δx) or vertical ($\Delta \ln P$) spatial separation,

$$\rho^{xy} = \exp\left[-\left(\frac{\Delta x}{D^{xy}}\right)^2\right] \quad (5)$$

$$\rho^z = \exp\left[-\left(\frac{\Delta \ln P}{D^z}\right)^{1.8}\right]. \quad (6)$$

Here $D^{xy} = 540$ km and $D^z = 0.38$ represent the horizontal and vertical (in log pressure) decorrelation scales for the first-guess error field and are broadly consistent with the error correlation models of Hollingsworth and Lonnberg (1986) and Goerss and Phoebus (1992). For a typical tropical profile, $D^z = 0.38$ corresponds to a decorrelation height of $\sim$3 km.

We note that under certain circumstances a formal solution of (4) yields a weight vector $\mathbf{w}_k$ that is numerically ill-behaved. That is, $\mathbf{w}_k$ may contain wildly varying values whose algebraic cancellation, when multiplied by the covariance matrix M, yields a poor approximation to the right-hand vector $\mathbf{h}_k$. Such behavior is not uncommon in the solution of a large number of linear equations, particularly if the covariance matrix M is near singular (Daley 1991). To alleviate this problem we solve (4) using the method of singular value decomposition (Press et al. 1987), which identifies the near-singular portions of the covariance matrix, enabling one to eliminate the ill-conditioned subspace of M. The read-

TABLE 1. The storms, number of cases, and forecast dates used for the CTRL and WIND experiments.

Name	No. of forecasts	Dates (MMDDHH)
Bertha (1996)	6	070800, 070812, 070900, 070912, 071000, 071012
Eduoard (1996)	10	082700, 082712, 082800, 082900, 082912, 083012, 090100, 090112, 090200, 090212
Fran (1996)	7	090200, 090212, 090300, 090400, 090412, 090500, 090512
Hortense (1996)	5	090512, 090600, 090700, 090712, 090800
Erika (1997)	14	090500, 090512, 090600, 090612, 090700, 090712, 090800, 090812, 090900, 090912, 091000, 091012, 091100, 091112
Bonnie (1998)	14	082200, 082212, 082300, 082312, 082400, 082412, 082500, 082512, 082600, 082612, 082700, 082712, 082800, 082812
Danielle (1998)	11	082500, 082512, 082600, 082612, 082700, 082712, 082800, 082812, 082900, 082912, 083000
Georges (1998)	23	091700, 091712, 091800, 091812, 091900, 091912, 092000, 092012, 092100, 092200, 092212, 092300, 092312, 092400, 092412, 092500, 092512, 092600, 092612, 092700, 092712, 092800, 092812
Ivan (1998)	5	092200, 092212, 092300, 092312, 092400
Jeanne (1998)	8	092500, 092512, 092600, 092612, 092700, 092712, 092800, 092812
Mitch (1998)	8	102500, 102512, 102600, 102612, 102712, 102900, 102912, 103012

er is referred to Press et al. (1987) and Daley (1991) for further details.

3. Impact of GOES winds on GFDL track forecasts

a. Overview of experiments

This section compares model forecasts integrated from two sets of experiments: a control run (CTRL) and an experimental run that includes the GOES winds (WIND). Except for the assimilation of the GOES winds, the model integrations for the CTRL and WIND experiments are identical in all other respects. A set of 111 cases are examined for 11 different Atlantic storms spanning three seasons. Table 1 lists the storm names and dates for the cases considered. Since the experiments were not performed in real time, the selection of the individual cases is based upon the availability of both satellite winds and NCEP analyses for initializing the model. For practical reasons, we also chose to avoid short-lived storms since they offer few cases for study. However, this may tend to bias our sampling toward stronger storms at the expense of weaker ones (e.g., tropical storms). For each case, 72-h forecasts are performed. The forecasted position (defined by the minima in the low-level pressure field) is recorded at 12, 24, 36, 48, and 72 h and compared with the observed track for each forecast period when a cyclone was of tropical storm strength or greater. The statistical significance of the CTRL and WIND integrations is evaluated using a modified Student's *t*-test as described by Franklin and De Maria (1992), assuming a 30-h separation between statistically independent forecasts.

b. Results for the 1996 Atlantic hurricane season

The observed (filled symbol) and model-predicted (open symbol) tropical cyclone tracks for 1996 are displayed in Fig. 2 for (Figs. 2a,b), Bertha, (Figs. 2c,d), Eduoard, (Figs. 2e,f), Fran, and (Figs. 2g,h) Hortense for both the CTRL (left) and WIND (right) experiments. For clarity, the observed storm location is plotted every 12 h while the predicted storm positions are only plotted for the 24-, 48-, and 72-h forecast positions. Inspection of Fig. 2 reveals that the assimilation of the GOES winds into the GFDL model results in a qualitative improvement in the forecasted tracks. In particular, the forecasts for Bertha, Eduoard, and Fran exhibit a more accurate forecast during recurvature in the WIND simulations compared to the CTRL. This reduces the westward bias in the predicted tracks, particularly for Eduoard and Fran, although a slight westward bias for the landfall of Hurricane Fran still persists in the WIND forecast. For Bertha and Hortense, the high variability in the early forecasts is reduced somewhat in the WIND experiments. It is also worth noting that the landfall positions for Hurricanes Bertha and Fran are both more accurate and have a smaller spread when the GOES winds are assimilated.

A quantitative evaluation of the impact of GOES winds on the GFDL forecasts is presented in Tables 2–5 for Bertha, Eduoard, Fran and Hortense, respectively. Each table lists the forecast position errors at 12, 24, 36, 48, and 72 h for the 1996 storms. The bold-faced numbers highlight the model with the smallest track error for each forecast period. To evaluate the skill of the GFDL forecasts, the relative forecast errors are computed with respect to CLIPER (a statistical regression model based upon climatology and persistence; Neuman

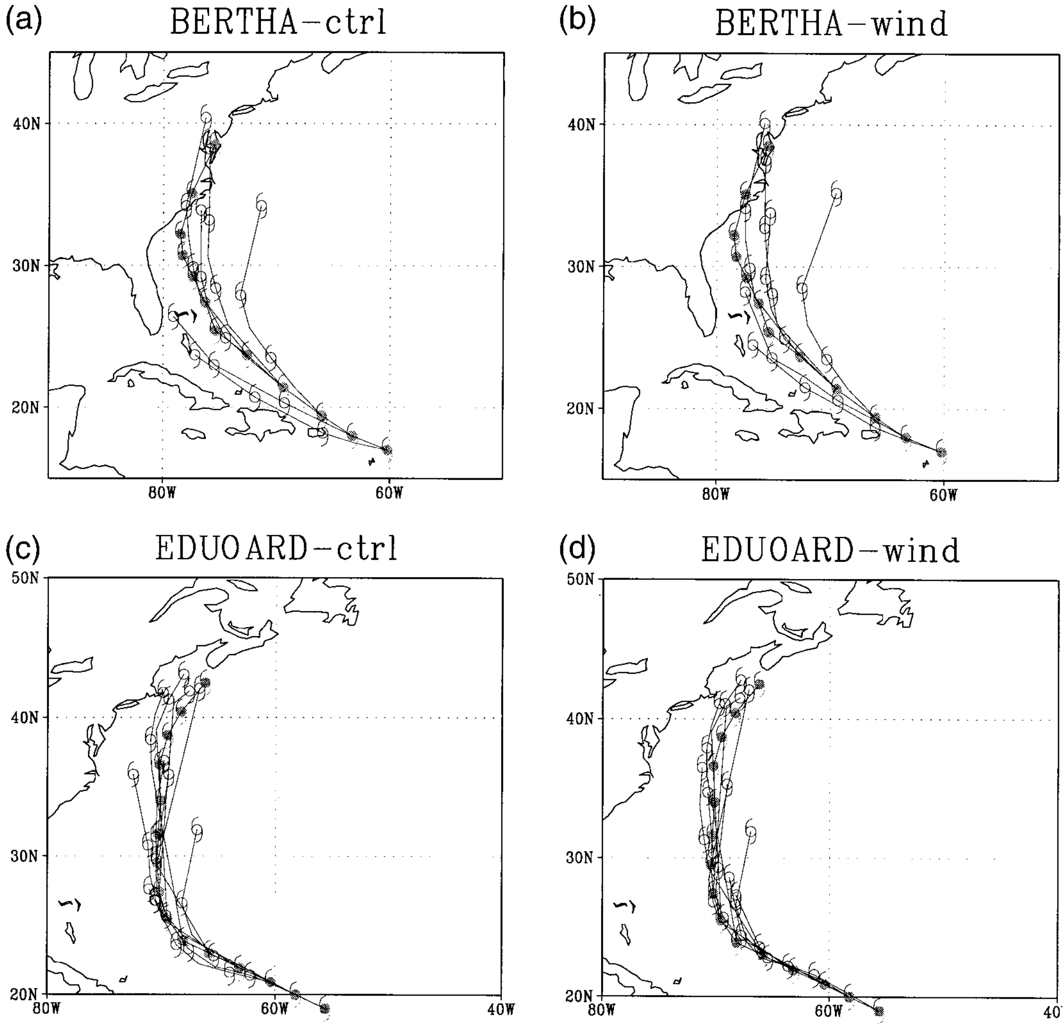

FIG. 2. A comparison of the observed track (filled symbol) with the forecasted positions from the CTRL (left) and WIND (right) forecasts for Hurricanes (a), (b) Bertha, (c), (d) Eduoard, (e), (f) Fran, and (g), (h) Hortense. The observed storm locations are plotted every 12 h. For clarity, only the 24-, 48-, and 72-h forecast positions are shown for the predicted tracks. Refer to Table 1 for forecast dates.

and Pelissier 1981) for both the CTRL and WIND experiments. Note that, for the vast majority of storms considered here, the CTRL experiments demonstrate substantial skill in track prediction relative to CLIPER. A more detailed evaluation of the performance of the GFDL model can be found in Bender et al. (1993), Kurihara et al. (1995), and Kurihara et al. (1998). For Hurricane Bertha, the assimilation of GOES winds reduces the mean track error for the GFDL model at all forecasts times, with the largest relative reductions occurring for the 12-h (14%) forecasts. For Eduoard, the wind assimilation reduces the track errors for 12–48 h, with a modest increase at 72 h. The impact on Fran is, in comparison, substantially larger. Track errors are unchanged for 12 h, while the 36–72-hour forecasts demonstrate track error reductions of 28%, 31%, and 26%, respectively. Some of the largest track error reductions for 1996 occurred for Hortense, where the 12–72-h track errors are reduced by 25%–38%. It is interesting to note that Hortense is also the storm for which the CTRL runs performed the worst with respect to CLIPER. Without the wind assimilation the GFDL model outperformed CLIPER for only one of the five forecast periods. In contrast, the model runs that included the GOES winds outperformed CLIPER at all five forecast periods. This suggests that an inaccurate analysis may be responsible for the relatively poor performance of the CTRL forecasts for this storm and that the assimilation of GOES winds substantially improved the accuracy of the initial conditions.

From the above analysis, it is clear that the impact of the GOES winds on the GFDL forecasts varies considerably from storm to storm. Furthermore, due to the relatively small number of cases for each storm, the level of statistical confidence in the results is also low. Therefore, to better assess the statistical significance of these

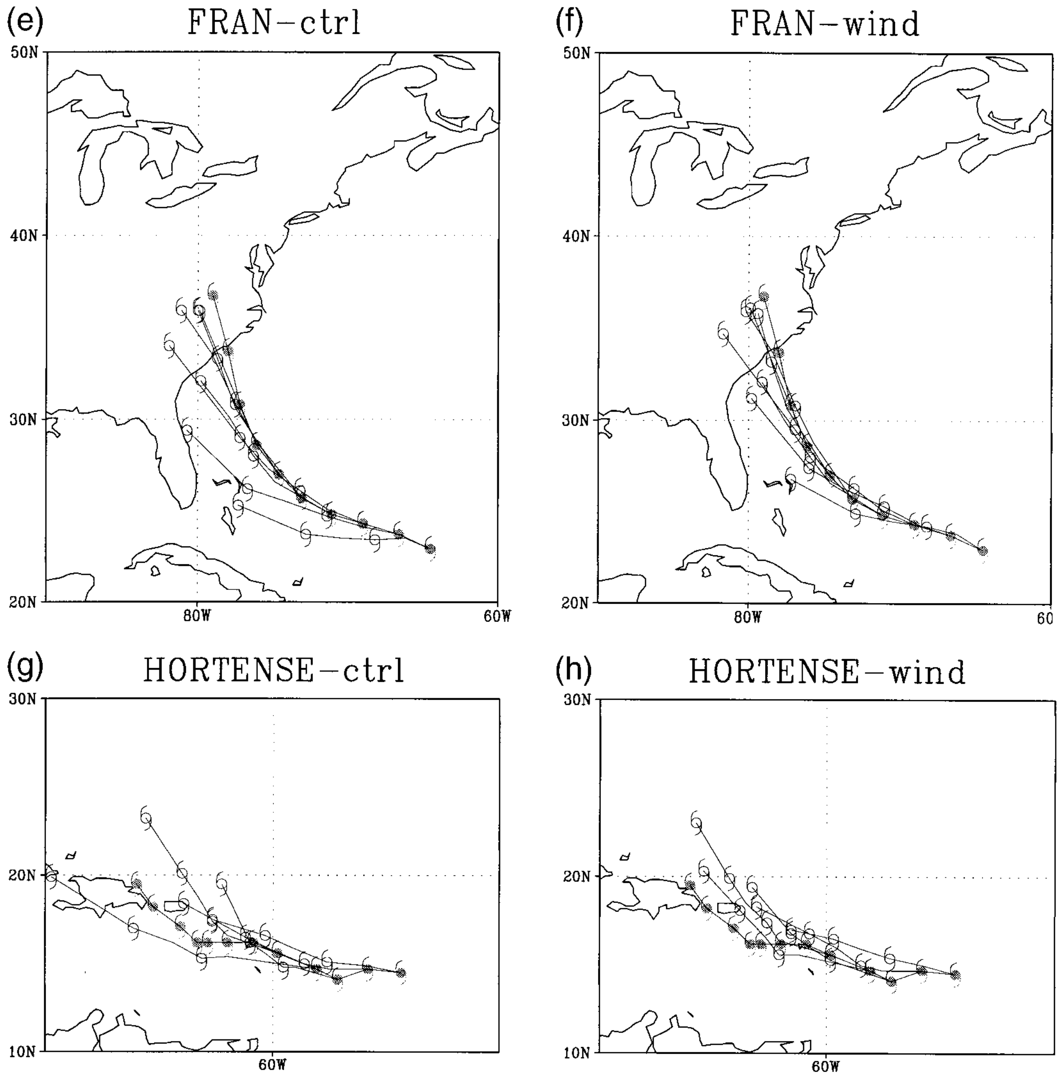

FIG. 2. (*Continued*)

experiments, a combined evaluation is performed using the results for all four 1996 storms. A graphical summary of this comparison is presented in Fig. 3. Overall, the WIND experiments for 1996 resulted in a reduction in mean track error for all forecast periods (Fig. 3, top). Track errors are reduced by approximately 15% for the 12- and the 36–72-h foreast periods, and by ∼10% for the 24-h forecast period. The 24- and 72-h forecast improvements are statistically significant at the 90% confidence level, while the 12-, 36-, and 48-h are statistically significant at the 95% confidence level. The combined error reductions, averaged over each of the five forecast periods, are statistically significant at the 99% confidence level. It is also useful to examine the percentage of forecasts that were improved when the satellite winds were included. This analysis (Fig. 3c) in-

TABLE 2. Comparison of average track errors (in km) from the CTRL, WIND, and CLIPER forecasts for Hurricane Bertha. The relative forecast errors with respect to CLIPER are shown in parentheses. Bold type highlights the smaller track error in each forecast period.

	N	CTRL	WIND	CLIPER
12 h	6	79 (−7%)	**68 (−20%)**	85
24 h	6	133 (−24%)	**130 (−25%)**	174
36 h	6	193 (−15%)	**193 (−15%)**	227
48 h	6	261 (−7%)	**260 (−7%)**	281
72 h	6	396 (−19%)	**373 (−23%)**	487

TABLE 3. Same as Table 2 except for Hurricane Eduoard.

	N	CTRL	WIND	CLIPER
12 h	10	57 (8%)	**55 (4%)**	53
24 h	9	97 (−6%)	**93 (−10%)**	103
36 h	8	122 (−34%)	**106 (−43%)**	185
48 h	7	137 (−51%)	**135 (−51%)**	277
72 h	6	**213 (−43%)**	232 (−38%)	374

TABLE 4. Same as Table 2 except for Hurricane Fran.

	N	CTRL	WIND	CLIPER
12 h	7	**42 (−25%)**	**42 (−25%)**	56
24 h	7	72 (−50%)	**69 (−52%)**	143
36 h	6	111 (−54%)	**80 (−67%)**	242
48 h	5	202 (−41%)	**141 (−60%)**	346
72 h	3	372 (−31%)	**278 (−49%)**	542

TABLE 5. Same as Table 2 except for Hurricane Hortense.

	N	CTRL	WIND	CLIPER
12 h	5	106 (23%)	**73 (−15%)**	86
24 h	5	167 (12%)	**125 (−17%)**	150
36 h	5	213 (5%)	**151 (−26%)**	203
48 h	5	258 (−5%)	**187 (−32%)**	272
72 h	5	403 (0%)	**253 (−38%)**	402

dicates that the assimilation of satellite winds led to a more accurate forecast in more than half of the cases, with the frequency of improved forecasts ranging from 50% (13 of 26 cases) at 24 h to 70% (14 of 20 cases) at 72 h.

c. Results for the 1997 Atlantic hurricane season

The 1997 hurricane season was relatively quiet with only one storm, Erika, that persisted long enough to provide a useful test of the GOES winds. Figure 4 compares the CTRL and WIND tracks with the observed tracks for 14 forecasts of Hurricane Erika. A distinct westward bias is evident in both the CTRL and WIND experiments. Comparison of the track error statistics (Fig. 5) is more revealing. For 12–36 h, the assimilation of satellite winds slightly increases the mean track error. However, these results are not statistically significant. At 48 h the satellite winds have a slight positive impact, and at 72 h the satellite winds have a very large positive impact (15% reduction in track error) that is statistically significant at the 99% confidence level. In addition, the assimilation of satellite winds improves 12 out of the 14 forecasts (86%) at 72 h.

It is interesting to note that both the 1996 and 1997 cases show statistically significant improvement for the 72-h forecasts, with relative improvements in track error of between roughly 15% and 20%. These results are consistent with the improvements obtained with the NOGAPS model (Goerss et al. 1998), which showed statistically significant track error reductions of ~12% at 72 h due to the assimilation of GOES winds. The improvement for the longer forecast period suggests that the satellite winds may be having the greatest impact on the environmental flow rather than the near-storm steering currents or that the correction of near-storm errors leads to reduced forecast error at future times. This may be partially attributable to the vortex bogusing procedure that filters out much of the smaller-scale circulation features near the storm center and replaces them with an idealized vortex (Bender et al. 1993). The spatial filtering, which is done after the satellite winds have been assimilated, negates much of the potential impact the satellite data might have on the near-storm circulation. While beyond the scope of the current study, future efforts will consider how the satellite winds can be used to improve the near-storm circulation, perhaps by including them as part of the vortex bogusing procedure.

d. Results for the 1998 Atlantic hurricane season

For the 1996 and 1997 hurricane seasons, the NCEP global analysis did not include any of the advanced GOES high-density wind observations produced by CIMSS. However, in 1998 NCEP began assimilating the GOES infrared (IR) winds operationally into their global forecast model, although the water vapor and visible winds were not assimilated during this period. Since the IR winds, which represent about 30% of the total number of wind vectors produced, have already been assimilated into the first-guess field via NCEP's variational analysis scheme (Parrish et al. 1997), one would expect the impact for 1998 to be somewhat less than that observed during the two previous years. Therefore the primary improvements for the 1998 WIND experiments relative to the CTRL should presumably reflect the information contained within the water vapor and visible winds (which were not assimilated by NCEP), as well as any additional weighting given to the IR winds in our analysis scheme. The IR winds are retained in the present assimilation since sensitivity tests indicate that their inclusion results in a modest (2%–3%) reduction in track error relative to WIND forecasts in which the IR winds are not reassimilated. While this reduction in error is too small to be statistically significant, it is consistent with the impression that IR winds are underweighted in the NCEP analysis relative to other sources of observation.

Another difference in the first-guess field for 1998 relative to previous years is that, due to difficulties with the implementation of a new higher-resolution analysis/forecast model in the summer of 1998, the quality of the operational analysis and forecasts during this period was diminished. In response to this, NCEP implemented a corrected assimilation/forecast model in October of 1998. In addition, NCEP reanalyzed a portion of this period with the corrected system. In this study, we will consider cases from both the original and corrected set of NCEP analyses. For the storms listed in Table 1,

TABLE 6. Same as Table 2 except for Hurricane Erika.

	N	CTRL	WIND	CLIPER
12 h	14	**73 (−8%)**	74 (−7%)	79
24 h	14	**137 (−21%)**	146 (−15%)	172
36 h	14	**172 (−39%)**	185 (−35%)	284
48 h	14	221 (−49%)	**218 (−50%)**	433
72 h	14	393 (−51%)	**335 (−59%)**	808

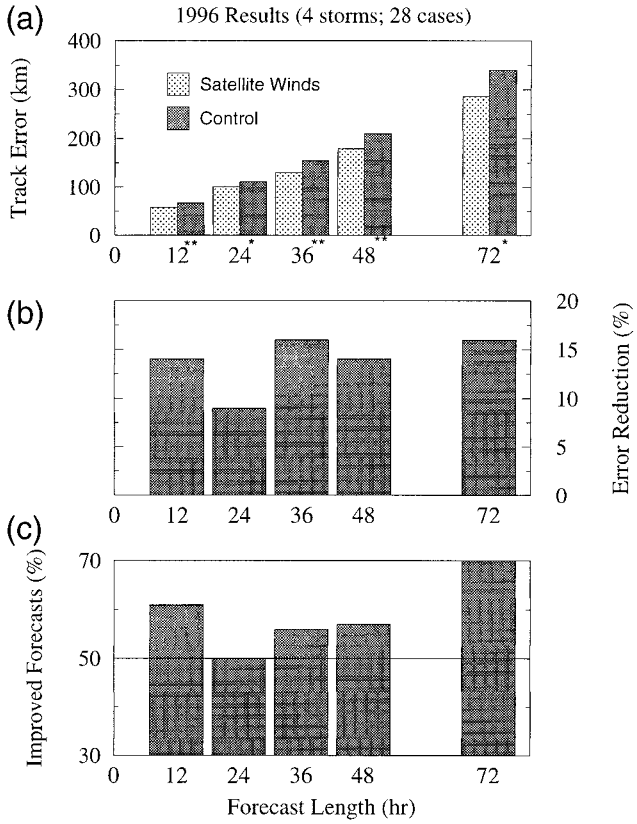

FIG. 3. Summary of the track errors from Bertha, Eduoard, Fran, and Hortense for 1996. (a) The mean track error, (b) the percentage reduction in track error, and (c) the percentage of improved forecasts due to the assimilation of GOES winds. The reductions in track error are statistically significant at the 95% confidence level for the 12-, 36-, and 48-h forecasts, and at the 90% confidence level for the 24- and 72-h forecasts. The error reduction averaged from all five forecast periods (12–72 h) is also statistically significant at the 99% confidence level.

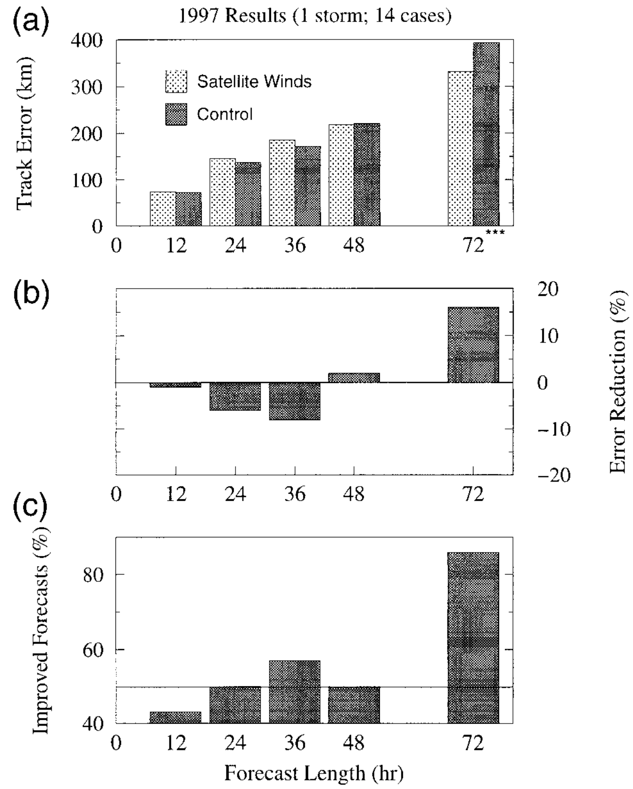

FIG. 5. Summary of the track errors from Hurricane Erika, consisting of (a) the mean track error, (b) the percentage reduction in track error due to the assimilation of GOES winds and the (c) percentage of improved forecasts due to the assimilation of GOES winds (bottom). The differences in track error are statistically significant at the 99% confidence level for the 72-h forecasts only.

forecasts for Bonnie and Danielle are based upon the reruns of the corrected NCEP analysis system; Georges, Ivan, and Jeanne are from the uncorrected operational system; and Mitch is from a corrected system that had

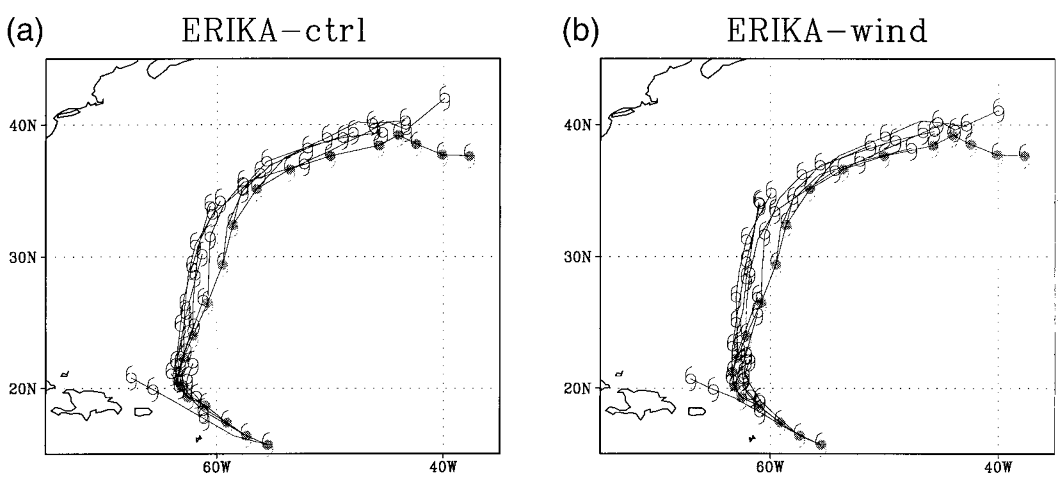

FIG. 4. A comparison of the observed track (filled symbol) with the forecasted positions from the (a) CTRL and (b) WIND forecasts for Hurricane Erika (1997). The observed storm locations are plotted every 12 h. For clarity, only the 24-, 48-, and 72-h forecast positions are shown for the predicted tracks. Refer to Table 1 for forecast dates.

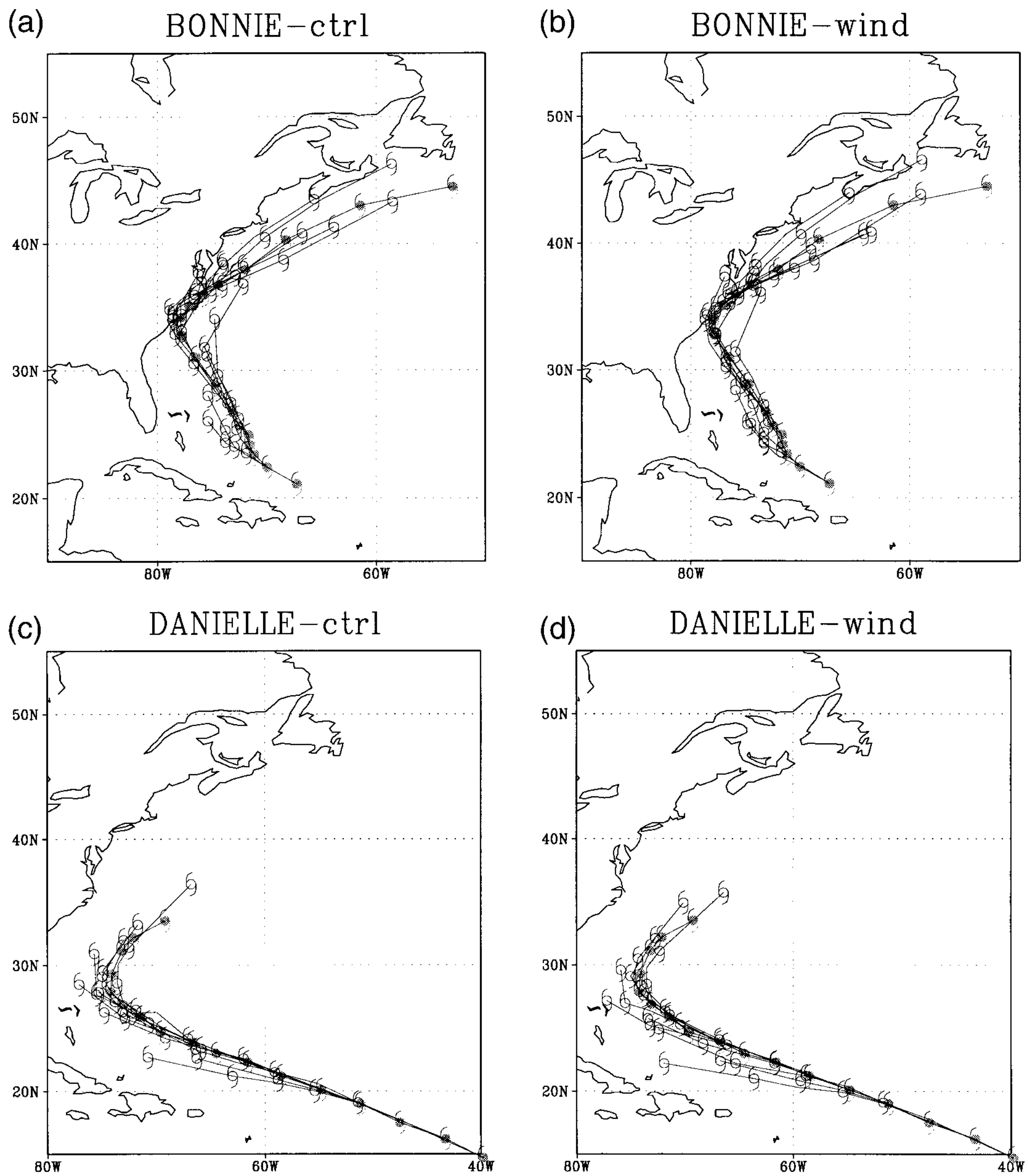

FIG. 6. A comparison of the observed track (filled symbol) with the forecasted positions from the CTRL (left) and WIND (right) forecasts for Hurricanes (a), (b) Bonnie, (c), (d) Danielle, (e), (f) Georges, (g), (h) Ivan, (i), (j) Jeanne, and (k), (l) Mitch. The observed storm locations are plotted every 12 h. For clarity, only the 24-, 48-, and 72-h forecast positions are shown for the predicted tracks.

been implemented operationally by the time it formed. Of course, these are not ideal conditions for performing a controlled experiment. However, the resources required to rerun a corrected analysis for the entire season cannot be justified solely for the purpose of this study. Thus, rather than ignore this season entirely, we have instead chosen to use the best NCEP analyses available for each storm, while acknowledging that the quality of the initial conditions may differ (for better or worse) during 1998 compared to previous seasons. It is largely for this reason that the data impact has been presented separately for each storm and each season. Yet, as demonstrated below, the model forecasts for 1998 are, like the previous two seasons, significantly improved following the assimilation of GOES winds.

For the 1998 season a total of 69 cases are considered from six different storms: Bonnie (14 cases), Danielle (11 cases), Georges (23 cases), Ivan (5 cases), Jeanne (8 cases), and Mitch (8 cases). The predicted tracks for these storms are shown for both the CTRL and WIND experiments in Fig. 6. A unique feature of this set of cases is that, with the exception of Georges, all of the

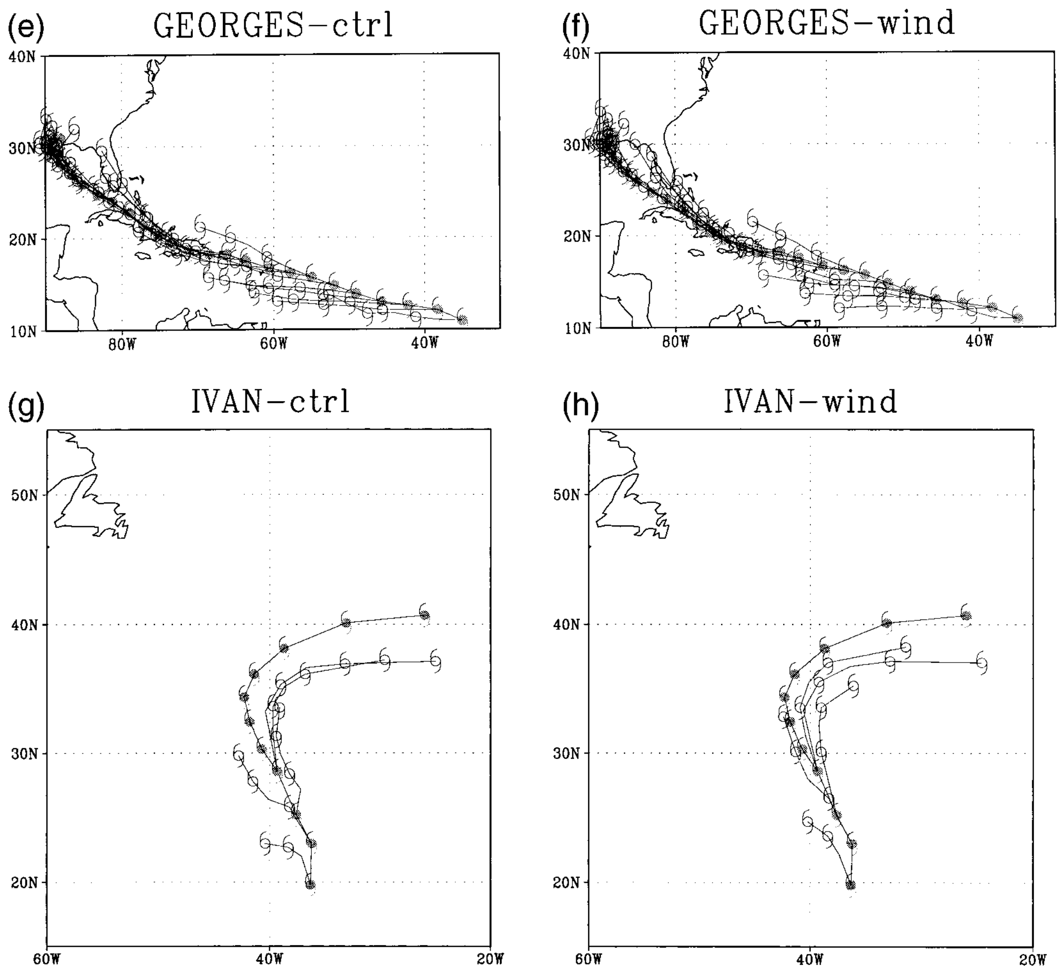

FIG. 6. (*Continued*)

storms exhibit a distinct recurvature at some point in their track. The WIND tracks from successive forecasts tend to be more consistent (less variable), relative to the CTRL. The greater consistency for the WIND experiments presumably reflects a convergence of the initial conditions toward the actual state of the flow field following the assimilation of the GOES winds.

Figure 7 shows the mean track errors composited from all five storms. On average, the assimilation of satellite winds improves the track forecasts for all verification periods. The track error reduction ranges from less than 5% at 12 h to nearly 15% at 24 and 36 h. The error reductions at 48 h are statistically significant at the 95% confidence level. The improvements at 24 and 36 h as well as the time-averaged (12–72 h) error reductions are statistically significant at the 99% confidence level. In addition to the mean track errors, the average performance of individual forecasts also improves following the assimilation of satellite winds. With the exception of the 12-h forecasts, the percentage of improved forecasts outnumber the percentage of degraded forecasts following the assimilation of satellite winds, with the frequency of improved forecasts ranging from 55% at 72 h to 67% at 24 and 48 h.

For 1998 there is again considerable variability from one storm to the next (e.g., Tables 7–12) and some indication that the impact of the satellite winds depends upon the quality of the background field use for the CTRL forecasts. For example, the forecasts for Ivan and Jeanne, which occurred in the central North Atlantic far from any conventional data sources, showed a substantially improved prediction of the recurvature following the assimilation of the satellite winds (Figs. 6g–j). Indeed, the largest track error reductions during 1998 were obtained for Ivan, which was well removed from the conventional observing network.

e. Composite analysis

The previous analyses have demonstrated that assimilation of the GOES winds leads to statistically significant improvements in the hurricane track predictions over multiple seasons. This improvement is also evident when comparing the cumulative performance of the

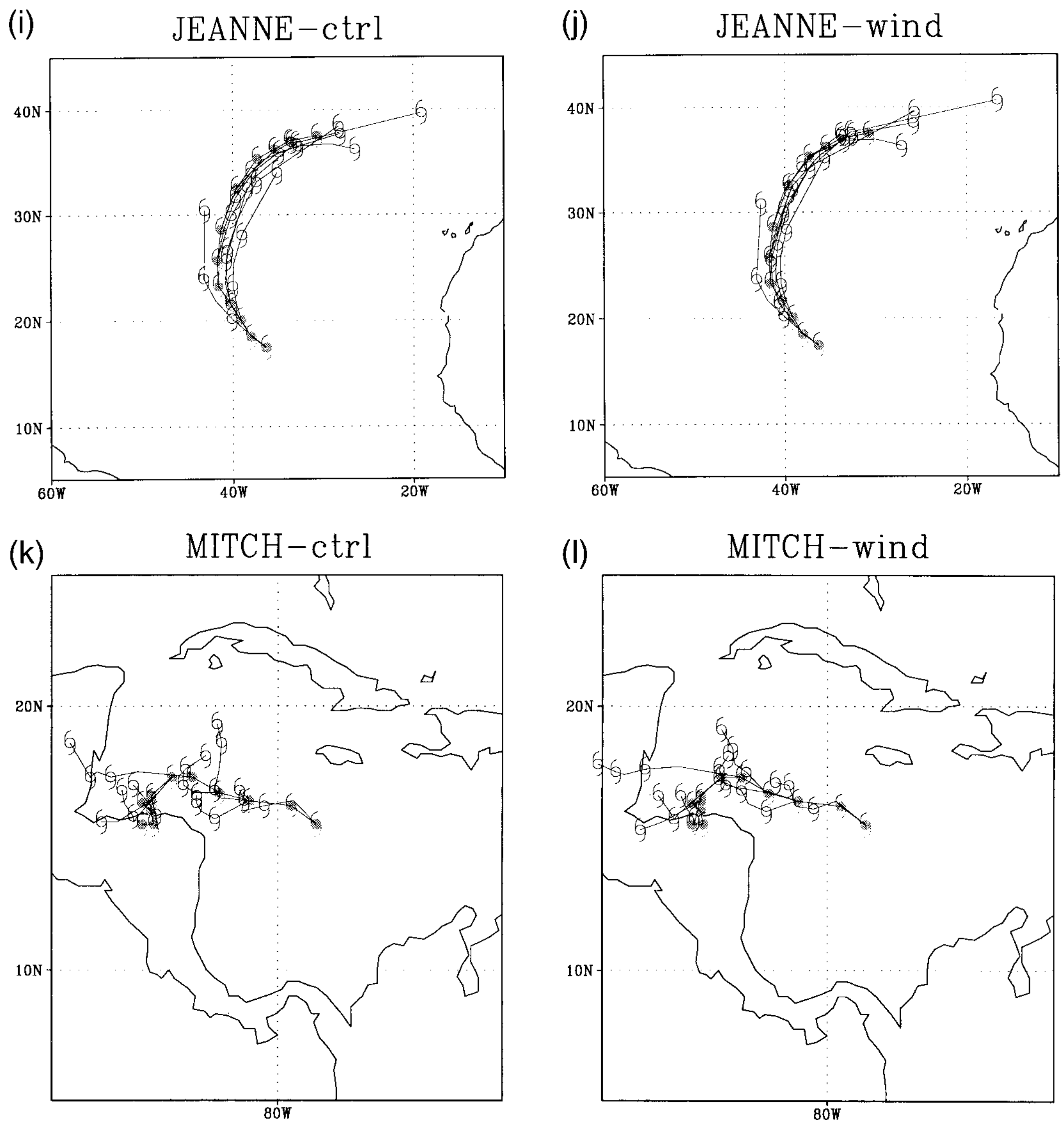

FIG. 6. (*Continued*)

WIND and CTRL experiments from all three seasons (Fig. 8). On average the assimilation of satellite winds improved forecasts for all verification times, with the reduction in track error ranging from 5% at 12 h to 12% at 36 h, with statistically significant reductions (99% confidence level) at 24, 36, and 48 h. The error reductions for the 12- and 72-h periods are significant at the 90% confidence level. With the exception of the 12-h forecasts, the inclusion of the satellite winds typically improved ~60% of the cases. These results offer compelling evidence of the ability of satellite-derived winds to significantly improve hurricane track forecasts and are consistent with the impacts reported by Goerrs et al. (1998) following the assimilation of GOES winds into the NOGAPS model.

While the statistical evaluations presented above demonstrate that the GOES winds lead to a significant reduction in forecasted track error, they offer little insight into why this improvement is obtained. That is, what aspects of the circulation fields are improved following the assimilation of GOES winds. While identifying the physical mechanisms responsible for the improvement is often difficult, such insight is important to fully understand the contributions of the GOES winds and can offer guidance to future data assimilation efforts. In addition, the identification of a physically coherent signature of the satellite data that is consistent with the improved tracks lends further credibility to the statistical evaluations of the error reductions.

To determine the impact of the satellite winds on the model flow fields, the initial wind conditions from the CTRL and WIND experiments are compared. Rather than examine the winds at individual model levels, we compute a deep-layer mean (DLM) flow, defined as the

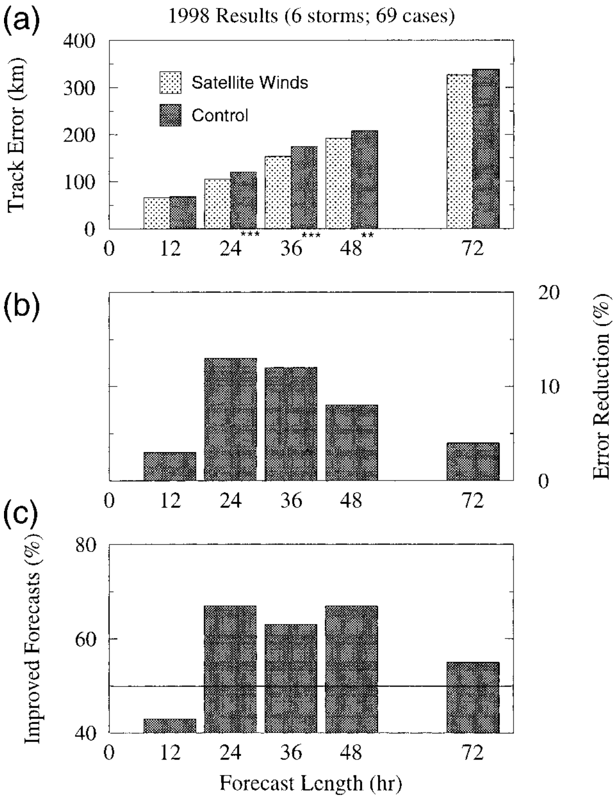

FIG. 7. Same as Fig. 3 except for 1998. The reductions in track error are statistically significant at the 99% confidence level for the 24- and 36-h periods, and at the 95% confidence level for the 48-h forecast period. The average error reduction for all forecast lengths (12–72 h) is also statistically significant at the 99% confidence level.

vertical pressure-weighted average of the initial condition wind field, for both the CTRL and WIND runs. To highlight the large-scale environmental or ''basic'' flow patterns, the DLM fields are then low-pass filtered to remove disturbances of less than ~1000 km (Kurihara et al. 1993). This is the identical filtering technique used in the initialization to separate the fields into their basic and disturbance components. Since there are over 100 cases, each with widely differing synoptic conditions, it is difficult to analyze each case individually and identify consistent features. Instead, we have the computed the average storm positions for each period (Fig. 9) and constructed a composite of the mean DLM flow fields (Fig. 10) in which the wind vectors are averaged using the storm center as the frame of reference.

Comparison of the mean forecast tracks for the CTRL and WIND experiments, from all 111 cases (Fig. 9a), provides a convenient summary of the improved performance of the track forecasts following the assimilation of GOES winds. The WIND forecasts clearly exhibit a tighter recurvature that, in turn, results in a marked reduction in the westward bias of the track forecasts (Fig. 9b). The enhanced northward movement of the WIND forecasts may have contributed to their improved recurvature by positioning the storms closer to the midlatitude westerlies. The bias in the CTRL forecasts is consistent with a westward track bias found for both model guidance and official NHC track forecasts for recent years (Kurihara et al. 1998). Hence it is worth noting that the westward bias, which has been a persistent feature of the GFDL model forecasts, is almost completely eliminated following the assimilation of satellite winds. This suggests that much of the historical westward bias of the model may be related to biases in the initial conditions rather than a deficiency in the model itself. Also note that the reduction in westward bias does occur at the expense of a slight increase in the meridional bias; however, the increase in meridional bias (relative to the CTRL) is much smaller and only occurs for the 72-h forecast, whereas the reduction in zonal bias is evident at all forecast times.

To examine the impact of the GOES data on the initial wind fields, Fig. 10 illustrates the time-mean composite of the mean DLM flow from the CTRL runs (left) and the difference in DLM flow field (WIND-CTRL) due to the assimilation of GOES winds (right). In both of these figures, the DLM flow is presented as vectors while the vorticity of the DLM vectors is depicted by shading. Recall that the composites are constructed from a storm-centered frame of reference, which on these figures corresponds to 0°N, 0°W. Note that we have not subtracted the storm motion vector from these DLM fields. While this does affect the vectors, it has no impact on the vorticity fields since the storm motion vector, by definition, has no rotational component. Hence the vorticity fields provide a more reliable interpretation of the

TABLE 8. Same as Table 2 except for Hurricane Danielle.

	N	CTRL	WIND	CLIPER
12 h	11	54 (15%)	**52 (9%)**	47
24 h	11	92 (27%)	**85 (16%)**	73
36 h	11	145 (8%)	**143 (7%)**	134
48 h	11	191 (−10%)	**187 (−13%)**	213
72 h	11	**304 (−22%)**	313 (−20%)	388

TABLE 7. Same as Table 2 except for Hurricane Bonnie.

	N	CTRL	WIND	CLIPER
12 h	14	**60 (−20%)**	63 (−16%)	75
24 h	14	92 (−48%)	**85 (−52%)**	178
36 h	14	123 (−61%)	**111 (−65%)**	315
48 h	14	156 (−67%)	**145 (−70%)**	474
72 h	14	**328 (−55%)**	348 (−45%)	730

TABLE 9. Same as Table 2 except for Hurricane Georges.

	N	CTRL	WIND	CLIPER
12 h	23	65 (14%)	**64 (12%)**	57
24 h	23	108 (0%)	**99 (−9%)**	108
36 h	22	150 (−6%)	**137 (−15%)**	161
48 h	21	181 (−17%)	**163 (−26%)**	219
72 h	19	270 (−16%)	**268 (−17%)**	320

TABLE 10. Same as Table 2 except for Hurricane Ivan.

	N	CTRL	WIND	CLIPER
12 h	5	152 (−3%)	**116 (−26%)**	156
24 h	5	299 (35%)	**215 (−3%)**	222
36 h	5	444 (29%)	**329 (−5%)**	345
48 h	4	465 (−9%)	**349 (−18%)**	427
72 h	4	519 (−15%)	**365 (−40%)**	610

TABLE 12. Same as Table 2 except for Hurricane Mitch.

	N	CTRL	WIND	CLIPER
12 h	8	**60 (−20%)**	69 (−8%)	75
24 h	8	114 (−29%)	**98 (−39%)**	160
36 h	7	187 (−27%)	**162 (−36%)**	255
48 h	7	280 (−26%)	**247 (−35%)**	376
72 h	5	389 (−40%)	**320 (−50%)**	642

vortex–environment interactions. A key feature in the CTRL DLM flow is the presence of a distinct gyre consisting of anticyclonic circulation to the northeast and cyclonic circulation to the southwest of the storm center (Fig. 10, left). These gyres result from the interaction between the storm's vortex and the environmental gradient of both planetary and relative vorticity (DeMaria 1985; Fiorino and Elsberry 1989; Willoughby 1995; Wu and Emmanuel 1995). In the Northern Hemisphere, the vortex circulation forces a streamfunction dipole with anticyclonic circulation to the northeast and cyclonic circulation to the southwest. In an idealized setting, the resulting vorticity dipoles induce a northwestward drift of the vortex that has been postulated to play an important role in determining the initial storm movement (Carr and Elsberry 1990).

While vorticity gyres are common features in numerical models, documenting their presence in nature has been hampered by the lack of sufficient observations and the complex flow in the storm environment (Franklin et al. 1996). A detailed analysis of gyres from the GOES winds is beyond the scope of our study; however, it is interesting to note that the difference in the vorticity of the DLM flow between the WIND and CTRL experiments also reveals a distinct dipole structure (Fig. 10b). The DLM flow for the WIND experiments reveals an enhanced gyre dipole with greater anticyclonic circulation to the northeast of the storm and greater cyclonic circulation to the southwest of the storm. This suggests that, while the initial wind field from NCEP does contain a gyrelike pattern, the strength of these gyres may be underanalyzed relative to that inferred from the GOES retrievals. However, the difference in vorticity fields does not form a pure SW–NE dipole structure, as would be expected from a simple β-gyre model, suggesting that vortex asymmetries and/or relative vorticity advection are also contributing factors. To the extent that a weaker gyre pattern is present, it would be consistent with the tendency for coarser-resolution models (such as that used to provide the CTRL initial conditions) to form a weaker storm circulation, which would, in turn, underpredict the advection of planetary and relative vorticity. The stronger northward flow that would be associated with an enhanced gyre structure agrees qualitatively with the northward displacement of the storm tracks in the WIND experiments relative to the CTRL (Fig. 9), although it does not offer an immediate explanation for the reduction in westward bias. However, the northward displacement of the storm may have contributed to the reduction in westward bias by accelerating the storm's movement toward the midlatitude westerlies. While this analysis cannot confirm that the possible presence of enhanced gyres is, by itself, responsible for the improved performance of the WIND forecasts, it does suggest that one advantage of the

TABLE 11. Same as Table 2 except for Hurricane Jeanne.

	N	CTRL	WIND	CLIPER
12 h	8	63 (−12%)	**62 (−14%)**	72
24 h	8	140 (−26%)	**126 (−33%)**	189
36 h	8	185 (−41%)	**166 (−47%)**	312
48 h	8	**204 (−54%)**	227 (−49%)	442
72 h	5	**306 (−59%)**	377 (−51%)	741

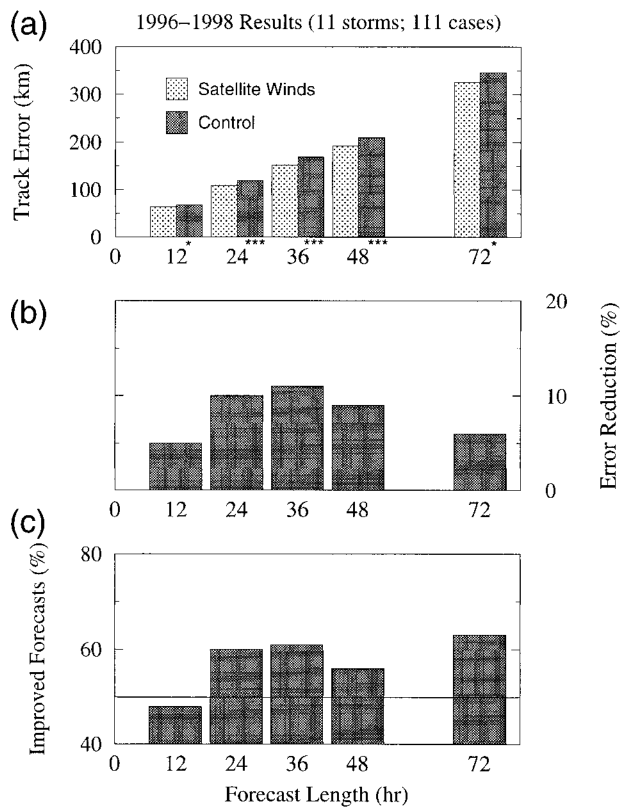

FIG. 8. Same as Fig. 3 except for all 111 cases from 1996 to 1998. The reduction in track error are statistically significant at the 99% confidence level for the 24-, 36-, and 72-h forecast periods, and at the 90% confidence level for the 12- and 72-h forecast periods. The average error reduction for all forecast lengths (12–72 h) is also statistically significant at the 99% confidence level.

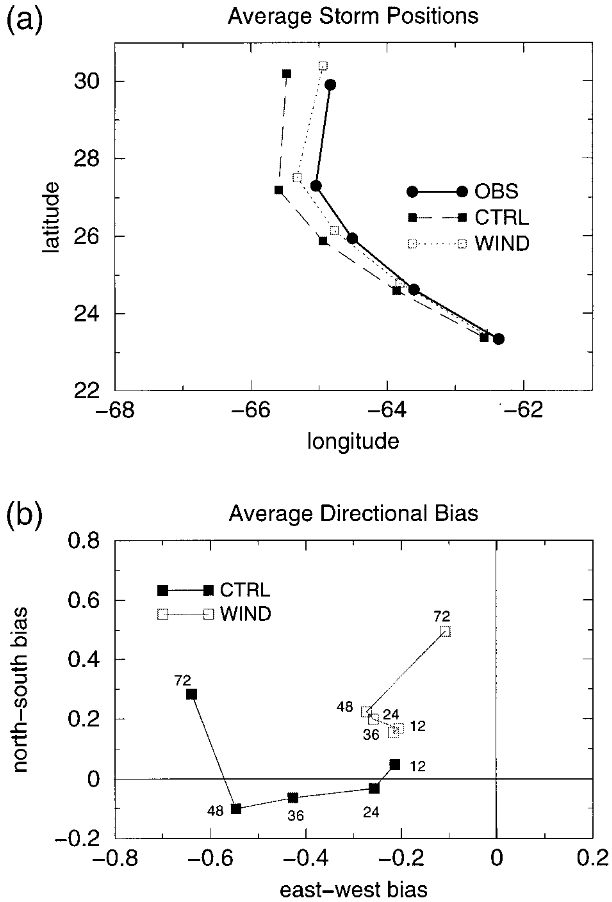

FIG. 9. The average storm tracks (top) from 1996 to 1998 (111 cases) for the observations (filled circle), CTRL forecasts (filled squares), and WIND forecasts (open squares). Results are plotted for the 12-, 24-, 36-, 48-, and 72-h forecast periods. The average directional bias between the model forecasts and observations is shown on the bottom.

GOES winds lies in their ability to observe the large-scale patterns of the horizontal vorticity in the environmental flow surrounding the storm. These results also support earlier studies with the GFDL model that suggested the importance of enhanced observations of potential vorticity in the upper troposphere for improved hurricane track forecasting (Wu and Kurihara 1996).

f. Dependence upon CTRL skill

Finally, we examine the extent to which the impact of the GOES winds depends upon the skill of the CTRL forecast. This analysis is motivated by the indication from sections 3b–3d and from previous studies suggesting that satellite winds may be particularly beneficial under the more difficult forecast situations. In particular, LeMarshall and Leslie (1998) demonstrated that satellite-derived cloud drift winds were capable of greatly improving the accuracy of track forecasts in cases where the conventional forecast guidance was poor. To explore this issue, the differences in track error between the WIND and CTRL forecasts ($\varepsilon_{\mathrm{WIND}} - \varepsilon_{\mathrm{CTRL}}$) are binned according to the relative error in the CTRL forecast computed with respect to CLIPER, $(\varepsilon_{\mathrm{CTRL}} - \varepsilon_{\mathrm{CLIP}})/\varepsilon_{\mathrm{CLIP}}$, where each bin has a width of 0.25. The results in each bin are compiled separately for each forecast period (12–72 h) and then averaged for all 111 cases. Figure 11 shows the mean difference in track error as a function of the relative error in the CTRL forecasts. Note that the degree of skill in the CTRL forecasts increases from right to left, with a relative error of -1 corresponding to a perfect CTRL forecast ($\varepsilon_{\mathrm{CTRL}} = 0$). For the majority of forecasts, the satellite winds reduce the track error; however, the magnitude and sign of the impact depends strongly on the skill of the CTRL forecast. Forecasts in which the CTRL track error is small $[-1 < (\varepsilon_{\mathrm{CTRL}} - \varepsilon_{\mathrm{CLIP}})/\varepsilon_{\mathrm{CLIP}} < -0.75]$ tend to be degraded by the assimilation of satellite winds, although this involved only a small percentage of the cases examined (~5%). On the other hand, the normalized skill score for the vast majority of forecasts (~70%) lies in the range, $-0.75 < (\varepsilon_{\mathrm{CTRL}} - \varepsilon_{\mathrm{CLIP}})/\varepsilon_{\mathrm{CLIP}} < 0$, which show systematic improvement following the assimilation of satellite winds. However, the most impressive impacts occur for those cases in which the CTRL forecasts exhibit little if any skill $[(\varepsilon_{\mathrm{CTRL}} - \varepsilon_{\mathrm{CLIP}})/\varepsilon_{\mathrm{CLIP}} > 0]$. In these cases, which compose approximately 25% of the total, the satellite winds offer substantial improvement in the forecast skill. As a result of these improvements, the number of forecasts that show no prediction skill relative to CLIPER is reduced by up to 20%. Thus, while the satellite winds typically improve the mean forecast error by ~10%, their impact does not occur uniformly, but rather is most pronounced for those cases in which the skill of the CTRL forecasts is lowest. This is consistent with the interpretation that forecasts with larger CTRL errors tend to be associated with a poorer specification of the initial conditions in the global analysis.

4. Summary

The prediction of hurricane tracks remains a challenging problem, particularly for recurving storms. Since improved track prediction depends heavily upon improved specification of the initial conditions, it is important to assess the impact of newly developed observation datasets, such as the experimental wind product derived from GOES observations at CIMSS (Velden et al. 1998). Recent enhancements in the wind retrieval algorithm and improved satellite instrumentation have provided unprecedented capabilities to observe the atmospheric circulation over the traditionally data-sparse tropical oceans with high spatial and temporal resolution. As shown here, the assimilation of these winds, even in a relatively simplified manner, is able to make a significant contribution to the reduction in track error. Moreover, this positive impact was obtained for a model

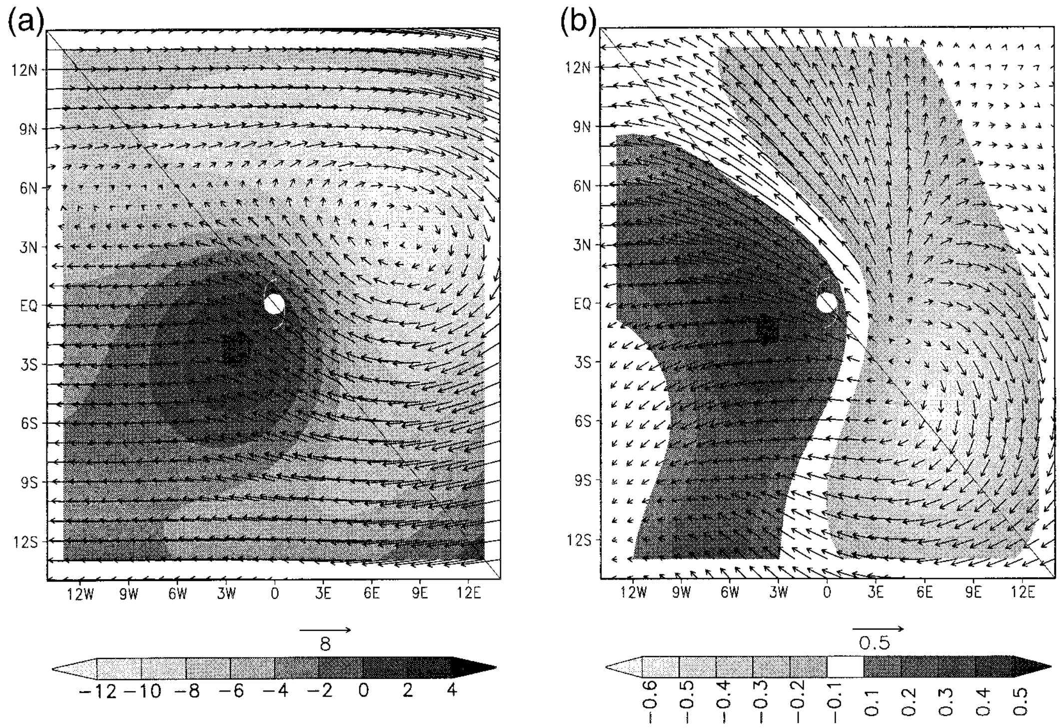

FIG. 10. A storm-relative composite of the large-scale steering flow from (a) the CTRL simulations and (b) the difference (WIND − CTRL) due to the assimilation of GOES winds averaged over all 111 cases. Vectors depict the deep layer mean winds (in m s^{-1}) and shading depicts the corresponding vorticity field (in 10^6 s^{-1}). The hurricane symbol identifies the center of the storm used as the frame of reference to form the multistorm composite.

with an outstanding forecast record (Kurihara et al. 1998). An additional strength of this study is the large number of experiments performed; over 100 cases were examined from 11 different storms covering three seasons (1996–98). Although the impact of the winds varied from storm to storm and from season to season, statistically significant reductions in the forecasted track error were obtained for all three seasons. Furthermore, when the entire set of experiments are considered, statistically significant improvements are obtained for all five forecast periods. The reduction in track errors ranged from 5% to 12% and roughly 60% of the forecasts were improved following the assimilation of satellite winds. However, the impact does not occur uniformly, but rather is most pronounced for those cases in which the skill of the CTRL forecasts is lowest. Indeed, track error reductions of up to 30%–40% were obtained for individual storms (i.e., Hortense and Ivan).

Analysis of the storm tracks indicated that assimilation of the GOES winds substantially improved the model forecasts of the storm recurvature. This improvement may have resulted from the ability of the GOES winds to more accurately depict the strength of vorticity gyres in the environmental flow. In particular, the difference in the vorticity of the DLM flow due to the assimilation of GOES winds exhibited a distinct dipole structure, consistent with an enhanced gyrelike structure. This indicates that, while the initial wind field used to perform the CTRL forecasts does contain a gyrelike structure, the strength of these gyres may have been underanalyzed relative to that inferred from the GOES retrievals. Such a bias is consistent with the tendency for coarser-resolution models to form a weaker storm circulation and thus underpredict the vorticity advection associated with the interaction between the storm and large-scale environmental flow.

It should be mentioned that the NCEP analysis, like all operational systems, undergoes periodic changes and improvements. Therefore past improvements from the satellite winds (or any other dataset) are no guarantee of future returns. For example, recent changes to NCEP's vortex analysis scheme for the 2000 season are expected to reduce track errors. Based upon Fig. 11, one might expect that as the quality of the NCEP analysis improves over time, the impact of the satellite winds (or other additional datasets) will be diminished. As a sensitivity study, a limited number of cases from Hurricane Gert were performed using NCEP reruns of the 1999 season with the new analysis scheme and positive impact of the satellite winds was obtained beyond 24 h. Although the magnitude of the reduction in track error (~5%) was less than the average improvement for 1996–98, it is not necessarily inconsistent with these results (i.e., Bonnie and Danielle had similar improvements). As the operational systems evolve over time,

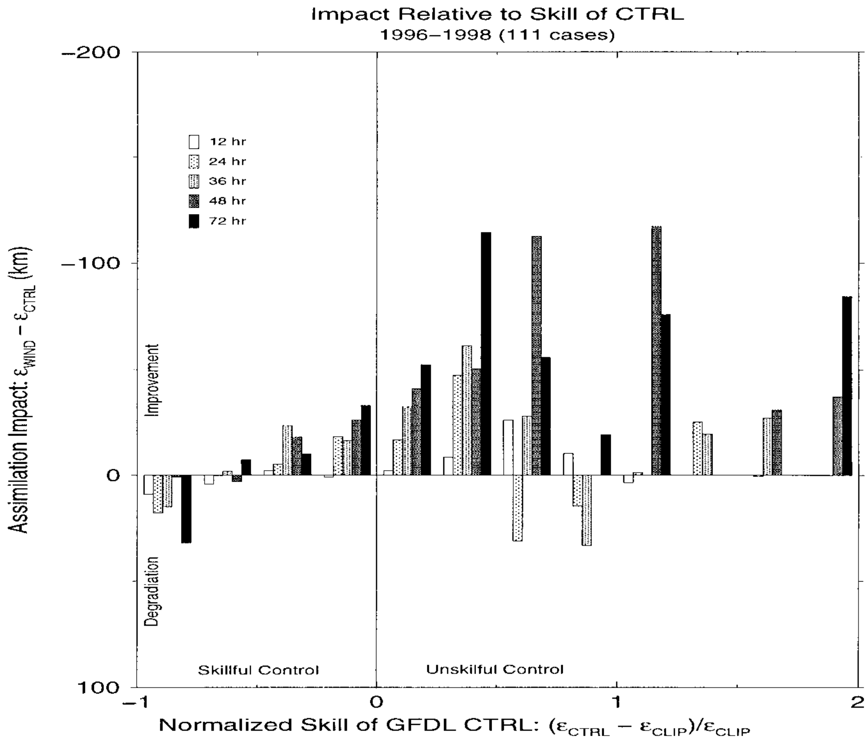

FIG. 11. A histogram of the impact of GOES winds as a function of the skill of the CTRL forecast. The differences in track error between the WIND and CTRL forecasts ($\varepsilon_{WIND} - \varepsilon_{CTRL}$) are binned according to the relative error in the CTRL forecast computed with respect to CLIPER, ($\varepsilon_{CTRL} - \varepsilon_{CLIP})/\varepsilon_{CLIP}$, where each bin has a width of 0.25. The results in each bin are compiled separately for each forecast period (12–72 h) and then averaged for all 111 cases. The skill of the CTRL forecast decreases from left to right, with a normalized skill score of -1 indicating a perfect CTRL forecast ($\varepsilon_{CTRL} = 0$). The approximate percentage of cases falling within selected intervals of CTRL skill are depicted on the graph with arrows. For the majority of forecasts, the satellite winds reduce the track error; however, the magnitude of the impact depends strongly on the skill of the CTRL forecast.

assessing the impact of satellite winds or any other dataset will require continual reevaluation.

While these results are encouraging, substantial work remains in this area and further improvements appear possible. In particular, the use of improved assimilation techniques, such as 4D variational analysis, which can utilize the high time resolution of the satellite data, are particularly promising (Leslie and LeMarshall 1998). In addition, more work is needed to better understand height assignments for clear-sky water vapor winds and to better define the nature of the model error covariances, which is critical to both 3D and 4D assimilation methods (Derber and Bouttier 1999). In the future, we hope to pursue such directions in collaboration with existing efforts both within the National Oceanic and Atmospheric Administration and abroad.

Acknowledgments. We thank Morris Bender, James Franklin, Matt Harrison, Tim Marchok, and John Molinari for their helpful comments and discussion. Steve Wanzong, Tim Olander, and Dave Stettner of CIMSS, and Jamie Daniels of NOAA/NESDIS, were helpful in obtaining the satellite wind fields. This work was partially supported by NOAA Grant NA67EC0100 to CSV.

REFERENCES

Aberson, S. D., and J. L. Franklin, 1999: Impact on hurricane track and intensity forecasts of GPS dropwindsonde observations from the first-season flights of the NOAA Gulfstream-IV jet aircraft. *Bull. Amer. Meteor. Soc.,* **80,** 421–427.

Bender, M. A., R. J. Ross, R. E. Tuleya, and Y. Kurihara, 1993: Improvements in tropical cyclone track and intensity forecasting using the GFDL initialization system. *Mon. Wea. Rev.,* **121,** 2046–2061.

Burpee, R. W., D. G. Marks, and R. T. Merrill, 1984: An assessment of omega dropwindsonde data in track forecasts of Hurricane Debby. *Bull. Amer. Meteor. Soc.,* **65,** 1050–1058.

——, J. L. Franklin, S. J. Lord, R. E. Tuleya, and S. D. Aberson, 1996: The impact of omega dropwindsondes on operational hurricane track forecast models. *Bull. Amer. Meteor. Soc.,* **77,** 925–933.

Carr, L. E., and R. L. Elsberry, 1990: Observational evidence for predictions of tropical cyclone propagation relative to environmental steering. *J. Atmos. Sci.,* **47,** 542–546.

Daley, R., 1991: *Atmospheric Data Analysis.* Cambridge University Press, 457 pp.

DeMaria, M., 1985: Tropical cyclone motion in a non-divergent barotropic model. *Mon. Wea. Rev.,* **113,** 1199–1210.
Derber, J., and F. Bouttier, 1999: A reformulation of the background error covariance in the ECMWF global data assimilation system. *Tellus,* **51A,** 195–221.
Fiorino, M., and R. L. Elsberry, 1989: Some aspects of vortex structure related to tropical cyclone motion. *J. Atmos. Sci.,* **46,** 975–990.
Franklin, J. L., and M. DeMaria, 1992: The impact of omega dropwindsonde observations on barotropic hurricane track forecasts. *Mon. Wea. Rev.,* **120,** 381–391.
——, S. E. Feuer, J. Kaplan, and S. Aberson, 1996: Tropical cyclone motion and surrounding flow relationships: Search for beta-gyres in an omega dropwindsonde dataset. *Mon. Wea. Rev.,* **124,** 64–86.
Gandin, L., 1963: *Objective Analysis of Meteorological Fields.* Israel Program for Scientific Translation, 232 pp.
Goerss, J. S., and P. A. Phoebus, 1992: The navy's operational atmospheric analysis. *Wea. Forecasting,* **7,** 232–249.
——, C. S. Velden, and J. D. Hawkins, 1998: The impact of multispectral *GOES-8* wind information on Atlantic tropical cyclone forecasts in 1995. Part II: NOGAPS forecasts. *Mon. Wea. Rev.,* **126,** 1219–1227.
Hollingsworth, A., and P. Lonnberg, 1986: The statistical structure of short-range forecast errors as determined from radiosonde data. Part I: The wind field. *Tellus,* **38A,** 111–136.
Kurihara, Y., M. A. Bender, and R. J. Ross, 1993: An initialization scheme of hurricane models by vortex specification. *Mon. Wea. Rev.,* **121,** 2030–2045.
——, ——, R. E. Tuleya, and R. J. Ross, 1995: Improvements in the GFDL hurricane prediction system. *Mon. Wea. Rev.,* **123,** 2791–2801.
——, R. E. Tuleya, and M. A. Bender, 1998: The GFDL hurricane prediction system and its performance in the 1995 hurricane season. *Mon. Wea. Rev.,* **126,** 1306–1322.
LeMarshall, J., 1998: Cloud and water vapor motion vectors in tropical cyclone forecasting. *Meteor. Atmos. Phys.,* **65,** 141–151.
——, and L. M. Leslie, 1998: Tropical cyclone track prediction using high resolution satellite data with a new methodology. *Aust. Meteor. Mag.,* **47,** 261–266.
Leslie, L. M., J. F. LeMarshall, R. P. Morison, C. Spinoso, R. J. Purser, N. Pescod, and R. Seecamp, 1998: Improved hurricane track forecasting from the continuous assimilation of high-quality satellite wind data. *Mon. Wea. Rev.,* **126,** 1248–1257.
Lord, S. J., 1993: Recent developments in tropical cyclone track forecasting with the NMC global analyses and forecasting system. Preprints *20th Conf. on Hurricanes and Tropical Meteor.,* San Antonio, TX, Amer. Meteor. Soc., 290–291.
Neuman, C. J., and J. M. Pelissier, 1981: Models for the prediction of tropical cyclone motion of the North Atlantic: An operational evaluation. *Mon. Wea. Rev.,* **109,** 522–538.
Parrish, D. F., J. C. Derber, R. J. Purser, W.-S. Wu, and Z. Pu, 1997: The NCEP global analysis system: Recent improvements and future plans. *J. Meteor. Soc. Japan,* **75,** 249–255.
Press, W. H., B. P. Flannery, S. A. Teuklolsky, and W. T. Vetterling, 1987: *Numerical Recipes.* Cambridge University Press, 818 pp.
Thiebaux, H. J., and M. A. Pedder, 1987: *Spatial Objective Analysis.* Academic Press, 299 pp.
Tuleya, R. E., and S. J. Lord, 1997: The impact of dropwindsonde data on GFDL hurricane model forecasts using global analyses. *Wea. Forecasting,* **12,** 307–323.
Velden, C. S., C. M. Hayden, W. P. Menzel, J. L. Franklin, and J. S. Lynch, 1992: The impact of satellite-derived winds on numerical hurricane track forecasting. *Wea. Forecasting,* **7,** 107–118.
——, ——, S. J. Neiman, W. P. Menzel, S. Wazong, and J. S. Goerss, 1997: Upper tropospheric winds derived form geostationary satellite water vapor observations. *Bull. Amer. Meteor. Soc.,* **78,** 173–195.
——, T. L. Olander, and S. Wazong, 1998: The impact of multispectral *GOES-8* wind information on Atlantic tropical cyclone track forecasts in 1995. Part I: Dataset methodology, description, and case analysis. *Mon. Wea. Rev.,* **126,** 1202–1218.
Willoughby, H. E., 1995: Normal-mode initialization of barotropic vortex motion models. *J. Atmos. Sci.,* **52,** 4501–4514.
Wu, C.-C., and K. Emmanuel, 1995: Potential vorticity diagnostics of hurricane movement. Part I: A case study of Hurricane Bob. *Mon. Wea. Rev.,* **123,** 69–92.
——, and Y. Kurihara, 1996: A numerical study of the feedback mechanisms of hurricane–environment interaction on hurricane movement from the potential vorticity perspective. *J. Atmos. Sci.,* **53,** 2264–2282.